

## Optical Characterizations of VCSEL for Emission at 850 nm with Al Oxide Confinement Layers

Merwan Mokhtari, Philippe Pagnod-Rossiaux, Francois Laruelle, Jean-Pierre Landesman, Alain Moréac, Christophe Levallois, Daniel Cassidy

► **To cite this version:**

Merwan Mokhtari, Philippe Pagnod-Rossiaux, Francois Laruelle, Jean-Pierre Landesman, Alain Moréac, et al.. Optical Characterizations of VCSEL for Emission at 850 nm with Al Oxide Confinement Layers. *Journal of Electronic Materials*, Institute of Electrical and Electronics Engineers, 2018, Special Section: 17th Conference on Defects-Recognition, Imaging and Physics in Semiconductors (DRIP XVII), 47 (9), pp.4987-4992. 10.1007/s11664-018-6221-x . hal-01861355

**HAL Id: hal-01861355**

**<https://hal-univ-rennes1.archives-ouvertes.fr/hal-01861355>**

Submitted on 14 Sep 2018

**HAL** is a multi-disciplinary open access archive for the deposit and dissemination of scientific research documents, whether they are published or not. The documents may come from teaching and research institutions in France or abroad, or from public or private research centers.

L'archive ouverte pluridisciplinaire **HAL**, est destinée au dépôt et à la diffusion de documents scientifiques de niveau recherche, publiés ou non, émanant des établissements d'enseignement et de recherche français ou étrangers, des laboratoires publics ou privés.

# Optical characterizations of VCSEL for emission at 850 nm with Al oxide confinement layers

MERWAN MOKHTARI<sup>1,2</sup>, PHILIPPE PAGNOD-ROSSIAUX<sup>1</sup>, FRANCOIS LARUELLE<sup>1</sup>, JEAN-PIERRE LANDESMAN<sup>2</sup>, ALAIN MOREAC<sup>2</sup>, CHRISTOPHE LEVALLOIS<sup>3</sup>, DANIEL T. CASSIDY<sup>4</sup>

1.- 3SP Technologies S.A.S, Route de Villejust, F-91625 Nozay Cedex, France. 2.- Univ Rennes, CNRS, IPR (Institut de Physique de Rennes) - UMR 6251, F-35000 Rennes, France. 3.- Univ Rennes, INSA Rennes, CNRS, FOTON - UMR 6082, F-35000 Rennes, France 4.- McMaster University, Department of Engineering Physics, 1280 Main Street West, Hamilton, Ontario, L8S 4L7; Canada.

Corresponding author: MERWAN MOKHTARI. -e-mail : [merwan.mokhtari@univ-rennes1.fr](mailto:merwan.mokhtari@univ-rennes1.fr) – Telephone: +33 2 23 23 47 29

## Abstract

In-plane micro-photoluminescence ( $\mu$ -PL) and micro-reflectivity measurements have been performed at room temperature by optical excitation perpendicular to the surface of two different structures: a complete vertical surface emitting laser (VCSEL) structure and a VCSEL without the upper  $p$ -type distributed Bragg reflector (P-DBR). The two structures were both laterally oxidized and measurements were made on top of oxidized and unoxidized regions. We show that since the photoluminescence (PL) spectra consist of the cumulative effect of InGaAs/AlGaAs multi quantum wells (MQWs) luminescence and interferences in the DBR, the presence or not of the P-DBR and oxide layers can modify significantly the spectrum.  $\mu$ -PL mapping performed on full VCSEL structures clearly shows oxidized and unoxidized regions that are not resolved with visible light optical microscopy. Finally, preliminary degree of polarization (DOP) of the PL measurements have been made on a complete VCSEL structure before and after an oxidation process. We obtain an image of DOP measured by polarization-resolved  $\mu$ -PL. These measurements allow us to evaluate main components of strain.

**Key words:** VCSELs, reliability, quantum well, oxide aperture, residual stress

## INTRODUCTION

Significant advances made in vertical cavity surface emitting lasers (VCSELs) emitting at 850 nm have increased the interest in high speed data communications applications, and particularly in data centers [1]. In this context, these laser diodes, which have been developed for commercial applications, are subject to very stringent performance and reliability requirements. These requirements have direct consequences on the geometry of the semiconductor laser diode, and particularly, specification of the multi quantum wells (MQWs) and cavity mirrors is crucial for good performance. In order to extract important operating parameters, different studies led by T. J. C. Hosea have been performed using spectroscopic characterizations as photo-modulated reflectance for retrieving the optical properties of VCSEL devices and the gain region [2-3]. Today, electrical and optical confinement is achieved by selective wet oxidation of  $\text{Al}_x\text{Ga}_{1-x}\text{As}$  ( $x>0.90$ ) layers within the VCSEL's vertical structure [4-5]. These aluminum oxide (AlOx) layers might constitute the main source of internal stress and these layers might be more critical since they are located close to the active area of the VCSEL [6-7]. Degradation mechanisms have been observed as extended dislocations originating from highly stressed areas pointing to the active region [8]. Much work has been done using different non-destructive strain measurements on AlOx confined structures [9-11].

In this work, in-plane micro-photoluminescence ( $\mu$ -PL) and micro-reflectivity measurements were realized along the vertical direction normal to the surface of VCSEL structures in order to characterize the active area. In a second part, preliminary degree of polarization (DOP) of the photoluminescence (PL) measurements have been made on the same complete VCSEL structures. Analysis of the DOP has been shown to be a useful technique for mapping the strain field owing to device processing in GaAs based materials [12]. These first measurements allowed us to evaluate the main components of strain induced by the critical steps of the manufacturing process of the VCSEL structures.

## EXPERIMENTAL

The samples for this study are VCSELs structures grown by metalorganic vapor phase epitaxy on (100) GaAs substrates for emission at 850 nm. The Si-doped lower DBR and the C-doped upper DBR are both made of pairs of  $\text{Al}_{0.12}\text{Ga}_{0.88}\text{As}$  /  $\text{Al}_{0.9}\text{Ga}_{0.1}\text{As}$ . The active region is undoped and consists of InGaAs/AlGaAs MQWs to obtain emission at 850 nm. On top of the active area, there are 2 or 4 layers, 15 to 30 nm thick, of  $\text{Al}_{0.98}\text{Ga}_{0.02}\text{As}$  for the oxide confinement. Following the epitaxial growth, the investigated samples were etched by inductively coupled plasma reactive ion etching in order to expose, on the mesa edges, the  $\text{Al}_{0.98}\text{Ga}_{0.02}\text{As}$  layers to oxidizing species. Rectangular and circular shapes of mesas were formed with dimensions from 20 to 250  $\mu\text{m}$ . Some samples were then laterally oxidized. The lateral extension of the  $\text{Al}_{0.98}\text{Ga}_{0.02}\text{As}$  oxidation was measured to be 30  $\mu\text{m}$  for the samples characterized by  $\mu$ -PL and micro-reflectivity and around 10 $\mu\text{m}$  for the samples characterized by DOP.

$\mu$ -PL measurements were performed at room temperature (RT) under excitation by a CW 633 nm laser source. The PL emission from the sample was collected through a 10 times microscope objective. The spectral resolution of the setup was 0.1 nm whereas the spatial resolution was 2 $\mu\text{m}$ . We inserted in the same optical set-up a white light source illuminating the sample perpendicular to its surface to perform reflectivity measurements.

DOP characterization was performed using 633nm excitation, at RT. Details on this technique can be found in [13]. We just recall here that the DOP signal measured along direction “y” can be written as:

$$\text{DOP}_y = \frac{L_x - L_z}{L_x + L_z} = -C_\epsilon (\epsilon_{xx} - \epsilon_{zz}), \quad (1)$$

where x and z denote the 2 directions perpendicular to y, and therefore belong to the plane of the surface being measured.  $L_x$  and  $L_z$  are the components of the spectrally-integrated PL with polarization along these 2 directions.  $\epsilon_{xx}$  and  $\epsilon_{zz}$  are the linear crystal deformations.  $C_\epsilon$  is a calibration constant which has been determined experimentally for some GaAs surfaces [12]. Note that in all the figures discussed here, x and z are the horizontal and vertical directions respectively. As shown in [13], the sensitivity of the DOP technique is such that deformations of  $10^{-5}$  can be detected. DOP is sensitive to non-biaxial deformations perpendicular to the beam propagation direction, so we can measure only anisotropic strain inside the structure.

## RESULTS AND DISCUSSION

A combination of in-plane  $\mu$ -PL with micro-reflectivity measurements on top of a periodic structure like VCSEL is very useful for understanding the  $\mu$ -PL spectra [14-15]. PL and reflectivity at RT in the in-plane geometry on top of unoxidized region from a complete VCSEL structure yield the spectrum shown in Fig. 1. For the reflectivity measurements we could not use a reference to normalize the intensity; the approach is then more qualitative than quantitative. We observe maxima in the wavelength range before 830 nm. Nevertheless, around 850 nm, where we expect the MQWs luminescence, we only measure a peak with a very low intensity. We can clearly see that a minimum of reflectivity corresponds to a maximum of PL. The luminescence of the  $\text{Al}_{0.12}\text{Ga}_{0.88}\text{As}$  layers from the P-DBR around 790 nm is filtered by the periodic structure of the VCSEL. The low intensity peak in the PL spectrum at 850 nm is at the same position as the dip in the reflectivity spectrum originating from the Fabry-Perot resonance of the cavity. This shows that most of the excitation is absorbed in the  $\text{Al}_{0.12}\text{Ga}_{0.88}\text{As}$  layers of the P-DBR so we don't excite too much the MQWs. This weak luminescence from the MQWs is then mostly filtered by the highly reflective P-DBR. In this configuration, we cannot determine the luminescence wavelength of the MQWs.

One way to characterize correctly the MQWs is by removal of the P-DBR [14]. We etched away most of the P-DBR layers and deposited a  $\lambda/4$  thick  $\text{SiN}_x$  layer acting as an anti-reflective coating in order to attenuate the dip of the half cavity. Fig. 2 shows that after etching away most of the P-DBR layers prior to wet oxidation, we can clearly see oxidized and unoxidized regions.

Fig. 3 shows the  $\mu$ -PL and micro-reflectivity spectra of the structure after the removal of most of the mirror layers. We observe that the dip corresponding to the mode of the cavity at 850 nm is now wider and shallower. This is the combined result of the P-DBR removal and the  $\text{SiN}_x$  layer deposited on top of the half cavity. The InGaAs/AlGaAs MQWs PL is now more intense and the real shape of the PL from the MQWs is now observable since a strong degradation of the cavity resonance has occurred. A determination of the PL wavelength is possible. This process can be useful in order to evaluate the PL wavelengths of the MQWs after the growth. However, this method is a destructive and time-consuming technique.

Next we studied the difference between oxidized and unoxidized regions on the complete VCSEL structure. We made both micro-reflectivity and  $\mu$ -PL measurements on top of the oxidized and unoxidized regions. Fig. 4a and 4b show respectively in-plane micro-reflectivity and  $\mu$ -PL both on top of oxidized and unoxidized regions. From the reflectivity spectra, we can observe that the dip corresponding to the mode of the cavity at 850 nm disappears from measurements on top of the oxidized region. From the  $\mu$ -PL spectra, we observe the same difference: the small peak corresponding to the MQWs luminescence disappears from measurements on top of the oxidized region. This is explained by the fact that after the oxidation of the  $\text{Al}_{0.98}\text{Ga}_{0.02}\text{As}$  layers into  $\text{AlO}_x$  layers, the refractive index of these layers is almost divided by 2. This process completely changes the cavity properties. In these oxidized areas, the cavity becomes anti-resonant and the resonant mode is then shifted out of the stop-band of the VCSEL.

Based on this observation and this difference between oxidized and unoxidized regions, we performed  $\mu$ -PL mapping on a large rectangular mesa and we then made a map of the integrated intensity of the MQWs. Fig. 5a and 5b show respectively the camera image of the sample and the corresponding  $\mu$ -PL mapping. We can clearly see oxidized and unoxidized regions that are not resolved with visible light optical microscopy. This method is a non-destructive technique that can be useful in order to identify oxidized and unoxidized regions through the surface.

Finally, we realized preliminary measurements of the DOP of photoluminescence on oxidized and unoxidized circular complete VCSELs structures.

For the unoxidized VCSEL structure, results are shown in Fig. 6. In this configuration, x and z are respectively the horizontal and vertical directions in the planes of the epitaxial layers. We observe that the highest values of DOP are located mainly close to the edges of the structure. Along the vertical axis (z direction), from the edge to the center of the mesa, we can see that the DOP is negative with a pronounced maximum value of the order of 8 % and then becomes positive and decreases. The same trend is observed along the horizontal axis (x direction) but with opposite sign of the DOP values. For a circular mesa, because of the symmetry, we could expect a circular distribution of the strain. Here, we can see that the symmetry is radial and it confirms the assumption. Based on that, along the horizontal axis (x direction) the DOP can be written as:

$$DOP_y = -C_\epsilon(\epsilon_{xx} - \epsilon_{zz}) = -C_\epsilon\epsilon_{xx} , (2)$$

Hence, along the horizontal axis, 8 % DOP converts into a linear deformation  $\epsilon_{xx}$  of the order of  $1.6 \times 10^{-3}$  (compressive deformation close to the edges). This strain measured in the structure is mainly due to the effect of the etching process that induces crystal deformations.

Fig. 7 shows the same measurements after the oxidation process. First, we observe on the PL map that the unoxidized window is not circular as expected but more like a “square shape”. This means that the oxidation reaction is not completely isotropic and the velocity of the reaction is different along specific crystallographic directions. Then, on the DOP map, we still have high values of DOP of the order of 10 % (absolute value) close to the edges of the mesa but we also measure strain close to the level of the oxidation fronts. We measure positive DOP along the horizontal axis (x direction) and negative along the vertical axis (z direction) both in the order of 1% (absolute value). These DOP measurements clearly show that the oxidation process induces some non-negligible anisotropic strain at the oxidation fronts in the VCSEL structure.

We performed in-plane micro-PL and micro-reflectivity measurements at RT on laterally oxidized VCSELs structures. We characterized the active area and we showed that since the PL spectrum consists of the cumulative effect of InGaAs/AlGaAs multi quantum wells (MQWs) luminescence and interferences in the DBR, the presence or not of the P-DBR and oxide layers can modify significantly the spectra. After removing most of the top mirror layers and then measuring the in-plane PL, characterization of the active region can be done. Finally, using polarization resolved  $\mu$ -PL, we realized preliminary DOP measurements on a complete VCSEL structure before and after oxidation. Signatures owing to strain inside the structure are clearly visible. We can see that the etching process and the oxidation process induce anisotropic strain that can be observed with this technique. Further improvements on DOP measurements, finite element simulations, and other characterizations will be investigated to evaluate, with accuracy, processing-induced defects for these components.

#### ACKNOWLEDGMENTS

This work was partly supported by the French RENATECH network and by the ScanMAT platform from Rennes 1 University.

#### REFERENCES

- [1] S. A. Blokhin, J. A. Lott, A. Mutig, G. Fiol, N. N. Ledentsov, M. V. Maximov, A. M. Nadtochiy, and V. A. Schchukin, and D. Bimberg, *Electron. Lett.* 45(10), 501-503 (2009).
- [2] T. J. C. Hosea, *Phys. Scr. T* 114, 227 (2004).
- [3] T. E. Sale, T. J. C. Hosea, and P. J. S. Thomas, *IEEE Photonics Technol. Lett.* 12(10), 1328-1330 (2000).
- [4] D. L. Huffaker, D. G. Deppe, K. Kumar, and T. J. Rogers, *Appl. Phys. Lett.* 65, 97 (1994).
- [5] K. D. Choquette, K. M. Geib, C. I. H. Ashby, R. D. Twesten, O. Blum, H. Q. Hou, D. M. Follstaedt, B. E. Hammons, D. Mathes, and R. Hull, *IEEE J. Sel. Top. Quant.* 3(3), 916-926 (1997).
- [6] K. D. Choquette, K. M. Geib, H. C. Chui, B. E. Hammons, H. Q. Hou, T. J. Drummond, and R. Hull, *Appl. Phys. Lett.* 69, 10 (1996).
- [7] C. Helms, I. Aeby, W. Luo, R. W. Herrick, and A. Yuen, *Proc. SPIE* 5364, 183–189 (2004).
- [8] R. W. Herrick, A. Dafinca, P. Farthouat, A. A. Grillo, S. J. McMahon, and A. R. Weidberg, *IEEE J. Quantum Electron.* 49(12), 1045-1052 (2013).
- [9] R. R. Keller, A. Roshko, R. H. Geiss, K. A. Bertness, and T. P. Quinn, *Microelectron. Eng.* 75(1), 96-102 (2004).
- [10] F. Chouchane, G. Almuneau, O. Gauthier-Lafaye, A. Monmayrant, A. Arnoult, G. Lacoste and C. Fontaine, *Appl. Phys. Lett.* 98(26), 261921 (2011).
- [11] J. P. Landesman, A. Fiore, J. Nagle, V. Berger, E. Rosencher, and P. Puech, *Appl. Phys. Lett.* 71(17), 2520-2522 (1997).
- [12] D. Lisak, D. T. Cassidy, and A. H. Moore, *IEEE T. Compon. Pack. T.* 24(1), 92-98 (2001).
- [13] D. T. Cassidy, S. K. K. Lam, B. Lakshmi, and D. M. Bruce, *Appl. Opt.* 43(9), 1811 (2004).
- [14] S. Gramlich, J. Sebastian, M. Weyers, and R. Hey, *Phys. Status Solidi A* 152(1), 293-301 (1995).
- [15] D. T. Schaafsma, D. H. Christensen, R. K. Hickernell, and J. G. Pellegrino, in *MRS Conference Proceedings* (1993), 326.

## FIGURE CAPTION

**Fig. 1.** In-plane PL (blue) and reflectivity (dashed red) spectrums from the complete VCSEL structure on top of the unoxidized region.

**Fig. 2.** In-plane view of rectangular mesas ( $550\ \mu\text{m} \times 230\ \mu\text{m}$ ) after etching and  $\text{SiN}_x$  deposition by visible light optical microscopy.

**Fig. 3.** In-plane PL (blue) and reflectivity (dashed red) spectrums from the half cavity on top of the unoxidized region.

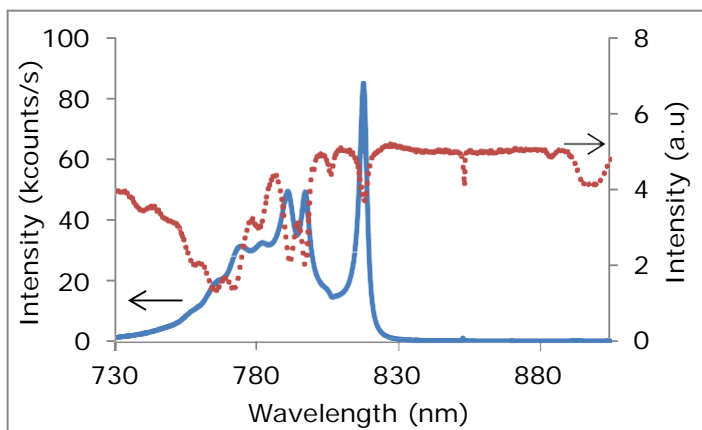
**Fig. 4.** In-plane micro-reflectivity (a) and  $\mu$ -PL (b) spectrums from the complete VCSEL structure on top of oxidized (black) and unoxidized (dashed red) regions. Inset shows the MQWs luminescence.

**Fig. 5.** (a) Camera image of two rectangular complete VCSEL structures ( $550\ \mu\text{m} \times 230\ \mu\text{m}$ ), including lateral oxidation. (b) Corresponding  $\mu$ -PL cartography of integrated intensity (in counts/s) of the QW luminescence. Bright and dark zones correspond respectively to the unoxidized and oxidized regions.

**Fig. 6.** Color scale maps of the DOP (a) and PL yield (b) for a  $25\ \mu\text{m}$  diameter circular unoxidized VCSEL structure. Measurements are along the normal to the (100) surface. Values for the DOP are indicated in % on the color scale to the right of the map. PL yield is given in counts (color scale to the right of the corresponding map).

**Fig. 7.** Color scale maps of the DOP (a) and PL (b) yield for a  $22\ \mu\text{m}$  diameter circular VCSEL structure after oxidation.

Fig1



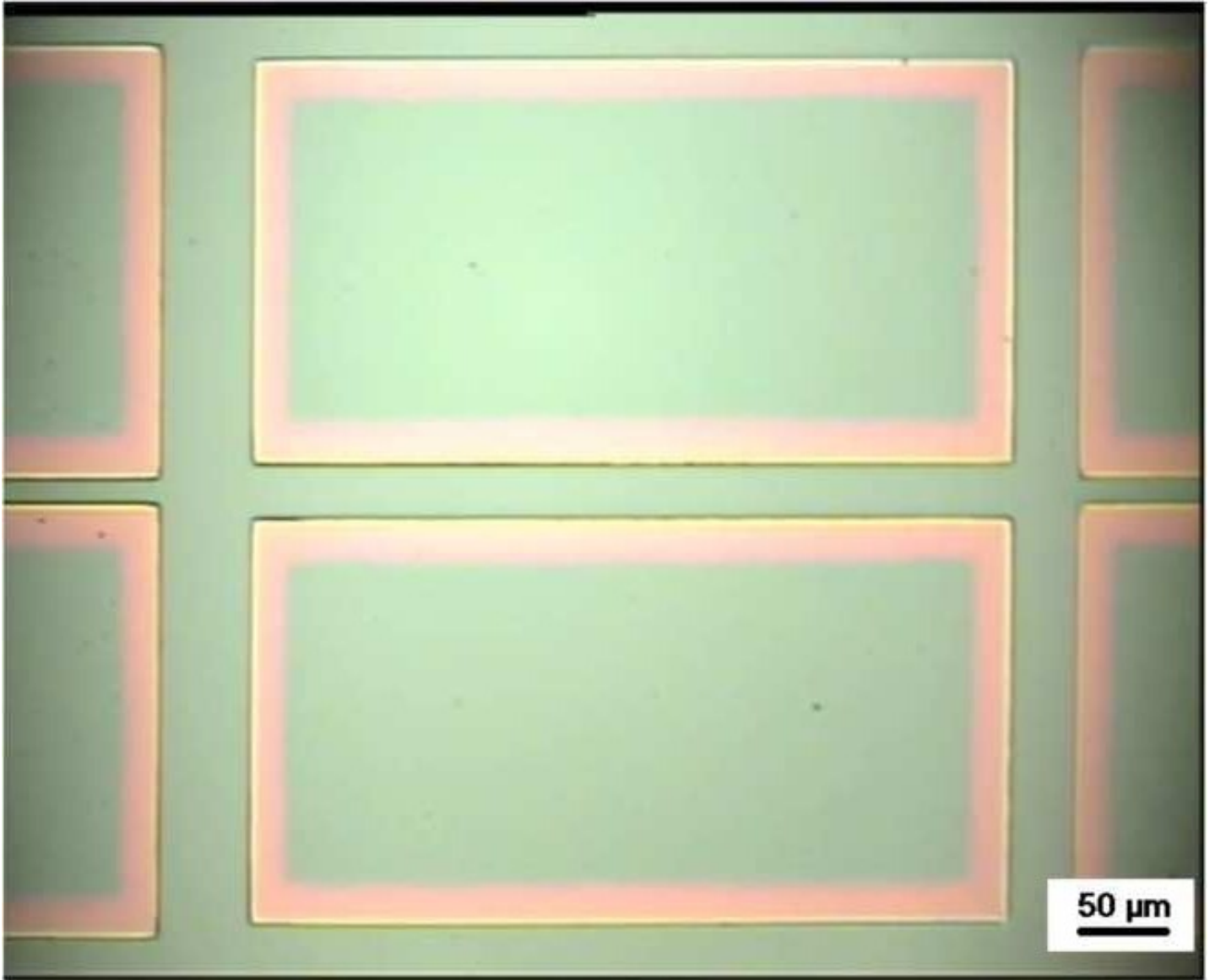


Fig3

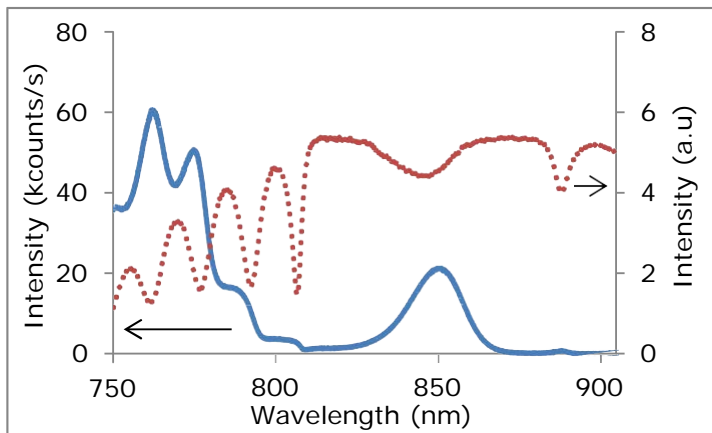
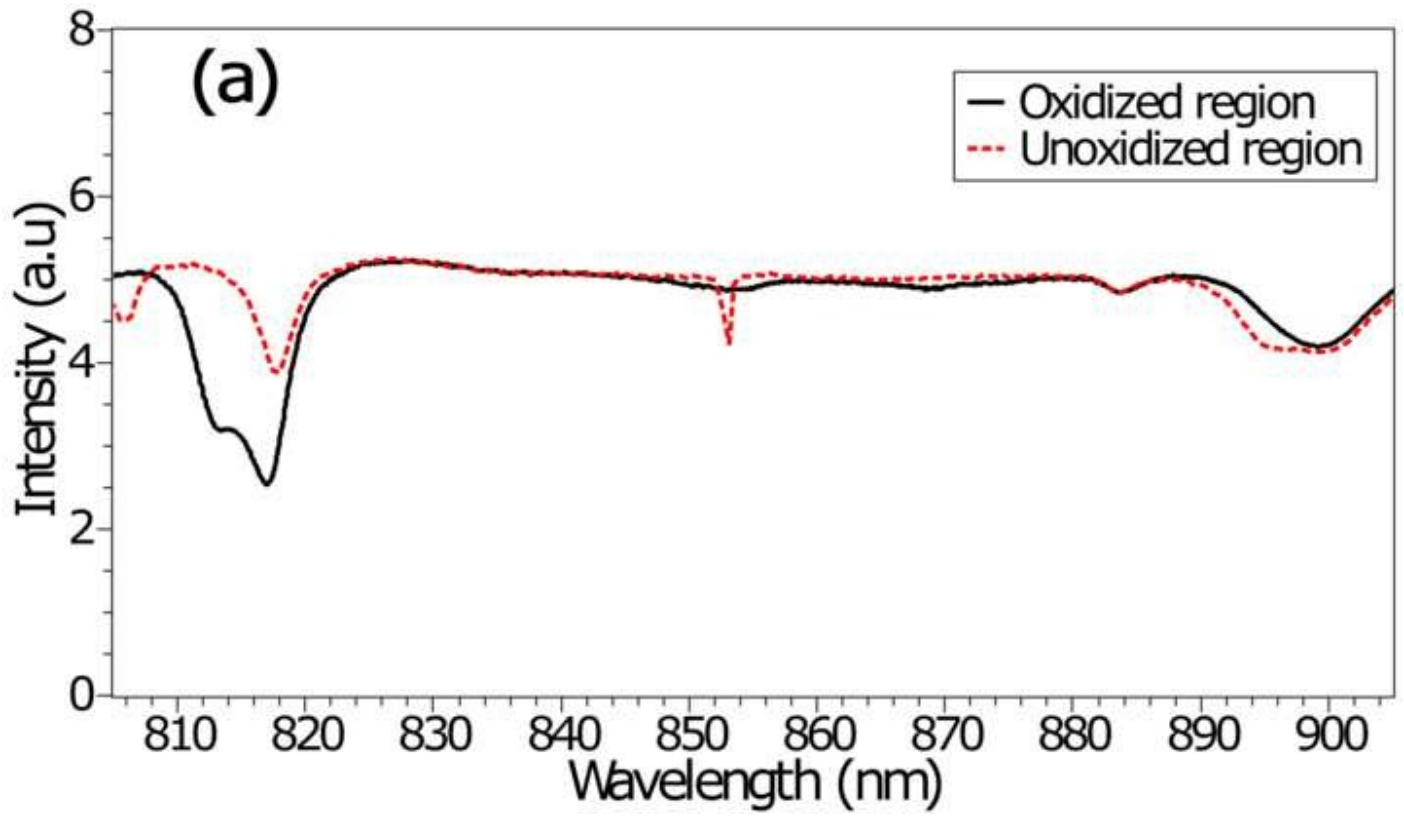


Fig4a



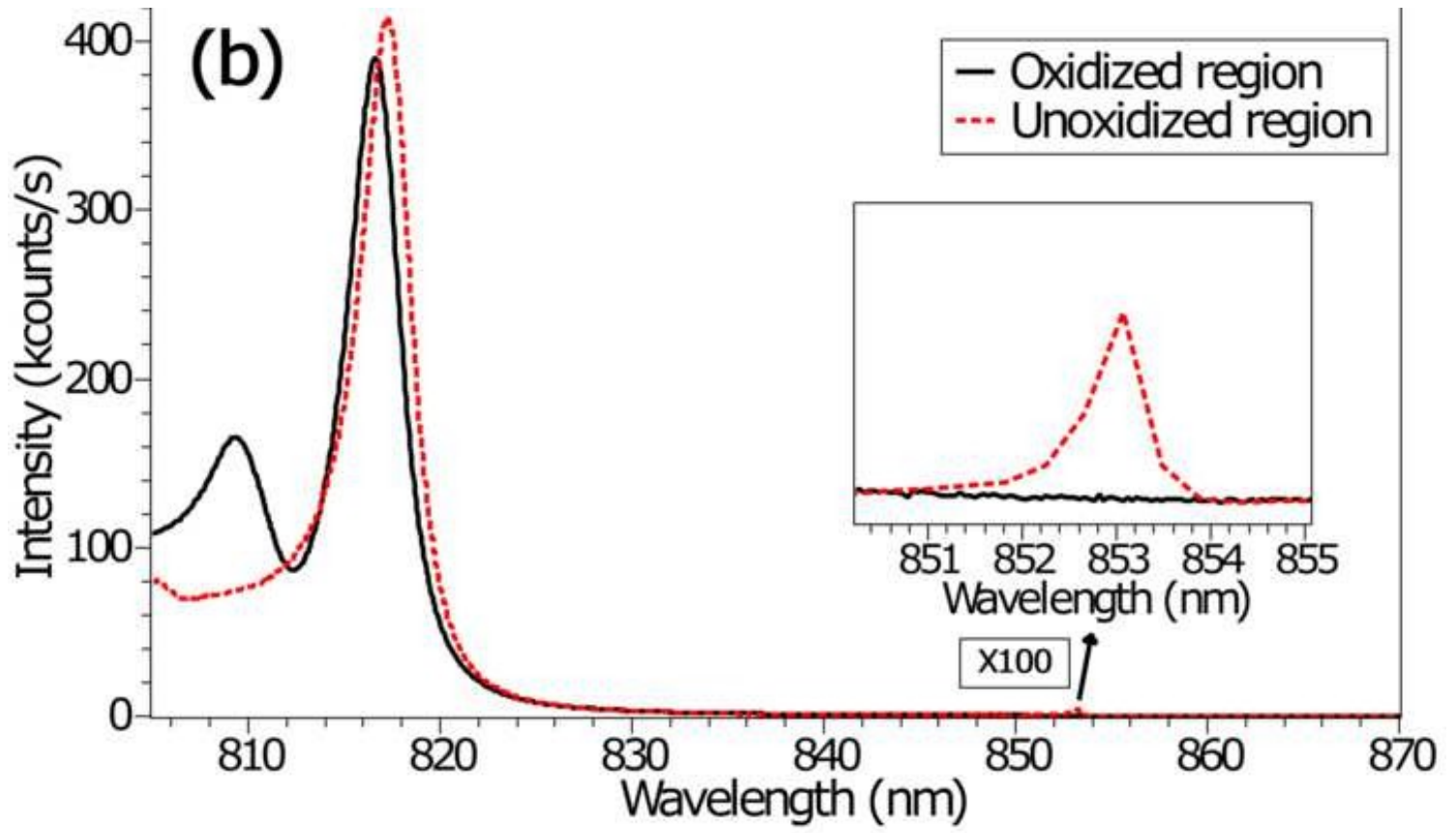


Fig5a

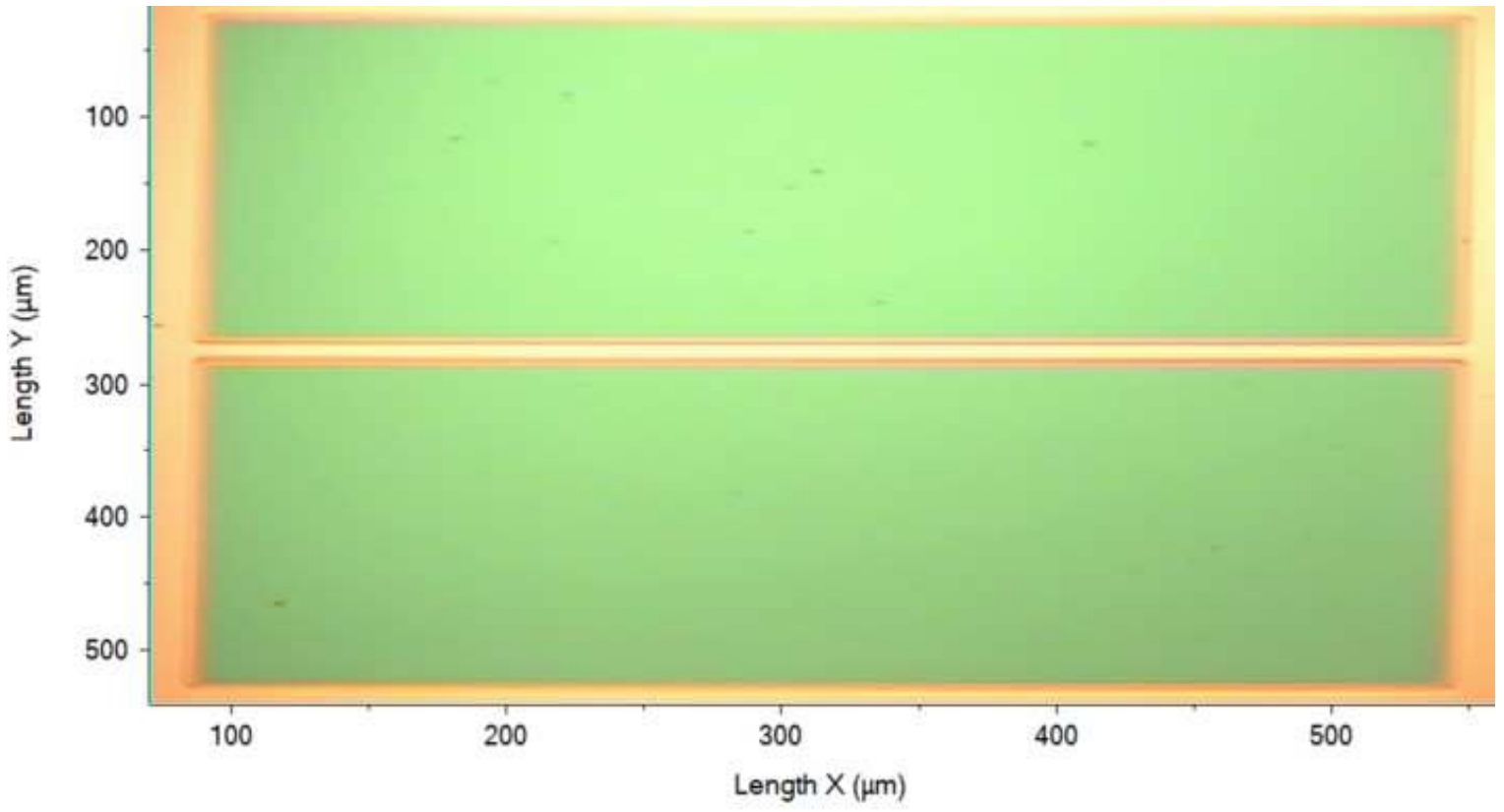
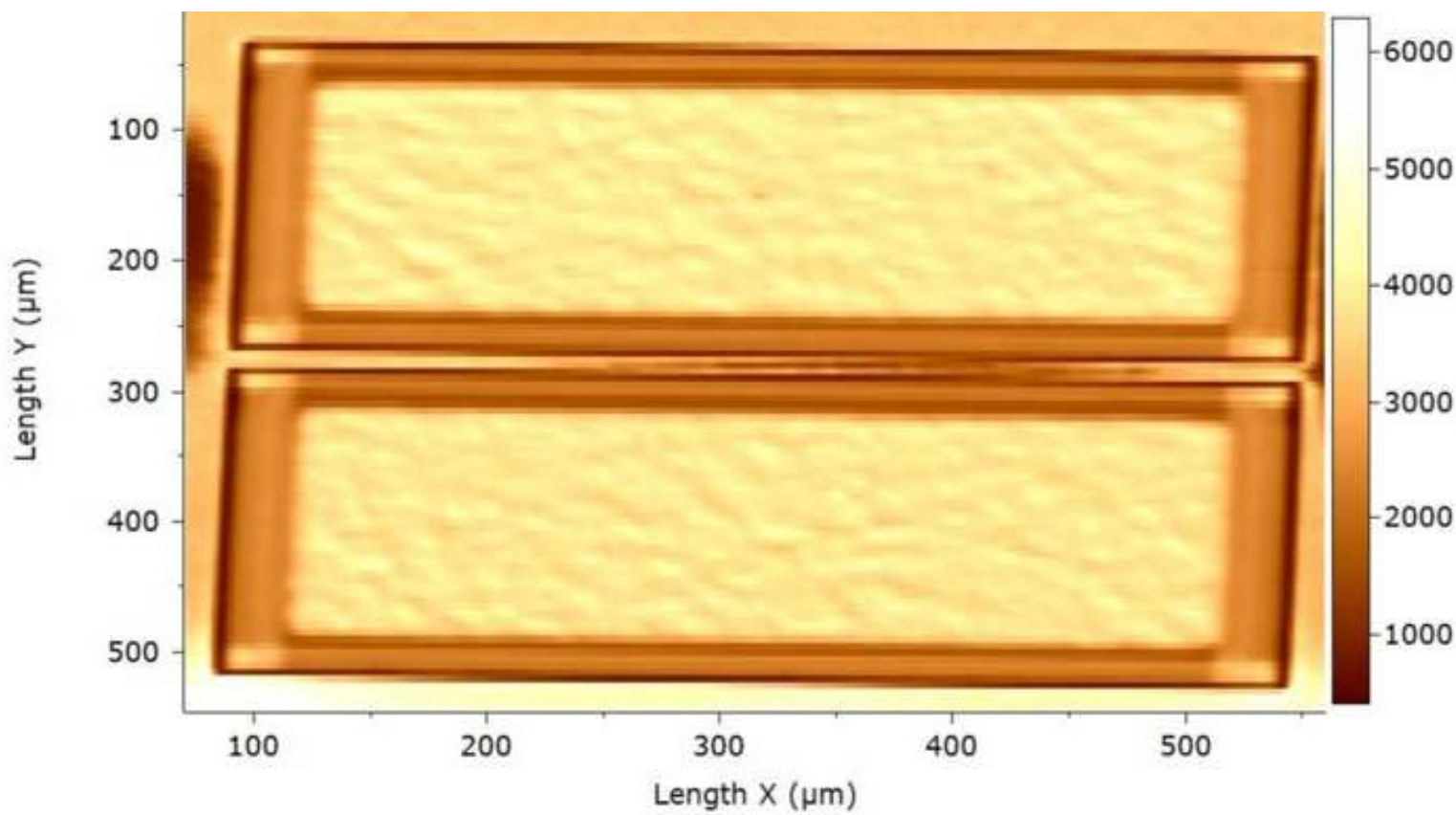
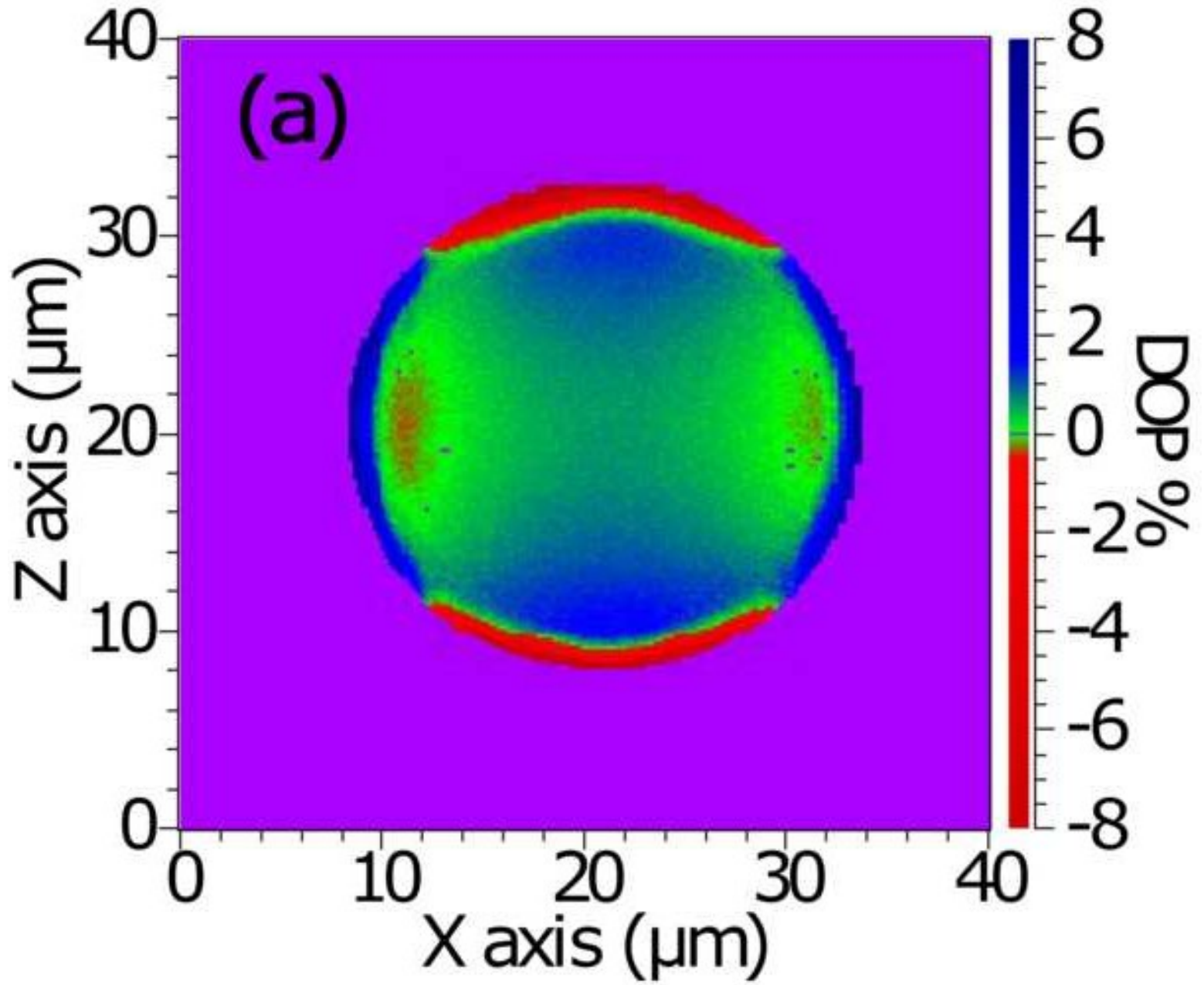
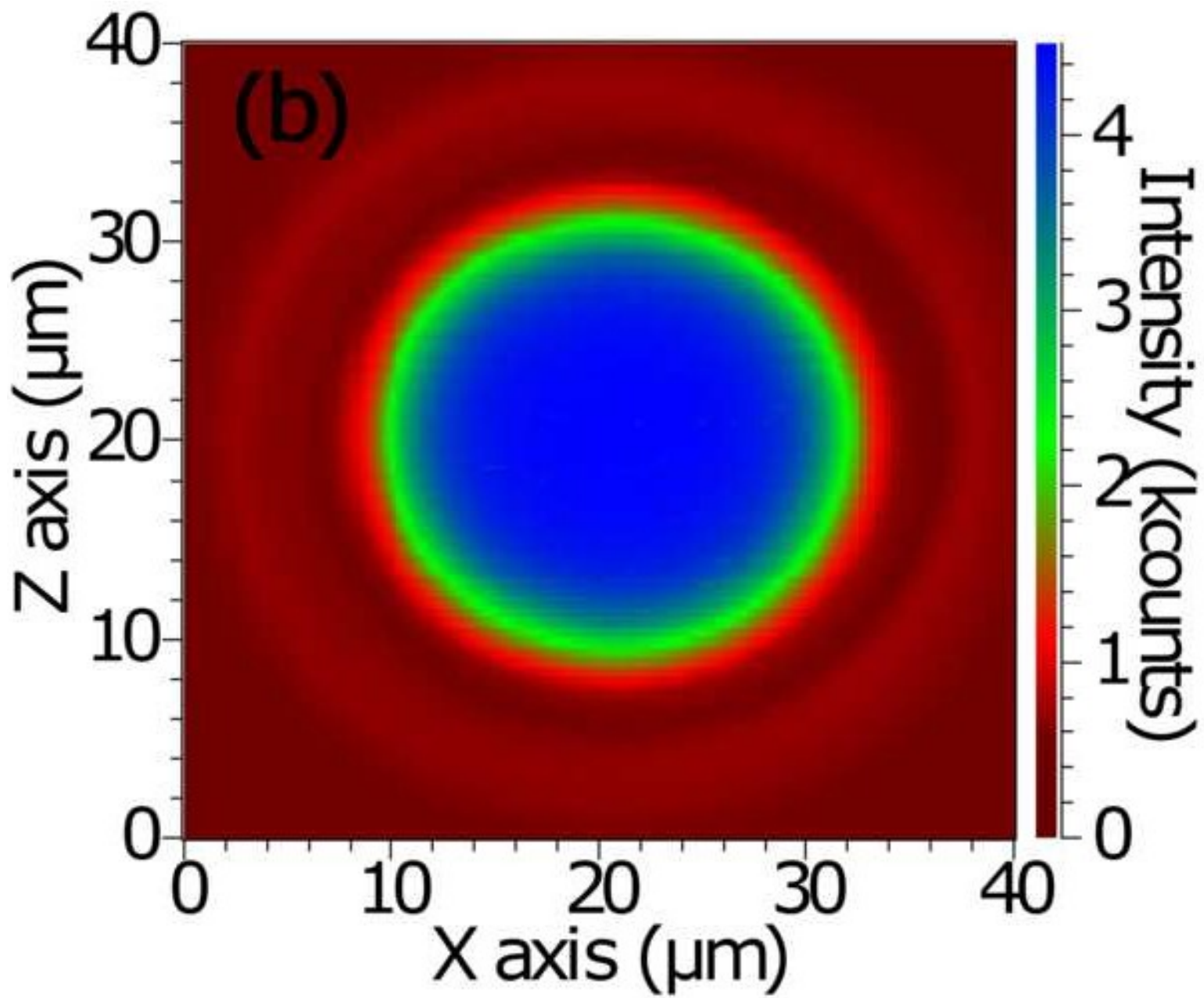


Fig5b

Fig5b







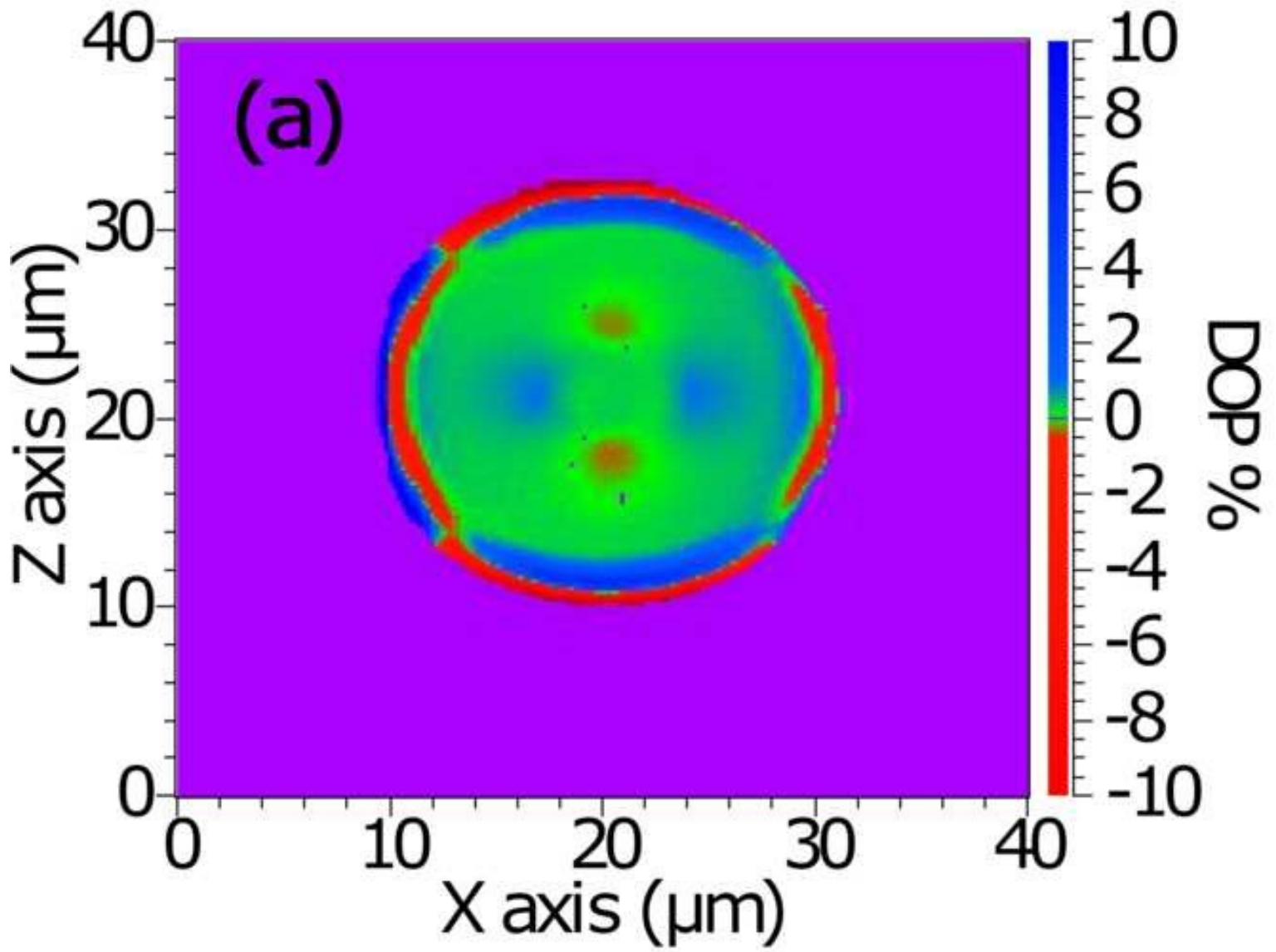


Fig7b

Fig7b

